AT&T Bell Laboratories Technical Journal
Vol. 63, No. 6, July–August 1984
Printed in U.S.A.

Transmission Errors in Companded PCM Over Gaussian and Rayleigh Fading Channels

By R. STEELE,* C.-E. SUNDBERG,† and W. C. WONG‡

(Manuscript received January 9, 1984)

Transmission errors in μ-law pulse-code-modulated systems are capable of inflicting considerable distortion in the recovered analog signals. We analyze this distortion when the transmission is over radio channels, and when either noncoherent frequency shift keying or coherent phase shift keying (CPSK) modulation is employed. We consider both Gaussian and Rayleigh fading channels, and for the latter we investigate the effect of bit scrambling prior to transmission and two types of diversity. We determined the gain in overall signal-to-noise ratio due to using the minimum distance code compared to the conventional folded binary code for low values of input signal power. In addition to the theoretical results, we present computer simulations of μ-law pulse-code-modulated encoded speech transmitted over the same channels, using CPSK modulation, bit scrambling, and diversity where appropriate, i.e., for the same conditions as employed in the derivation of our theory.

I. INTRODUCTION

Pulse Code Modulation (PCM) is well entrenched in the telephone networks as a means of conveying speech in a digital format,[1] and its impairments are therefore worthy of serious investigation. The distortion in the recovered speech signal arises from noise in the encoding process, and the presence of digital transmission errors. By employing logarithmic companded PCM at bit rates of 56 kb/s or 64 kb/s, and

* University of Southampton, England. † University of Lund, Sweden. ‡ AT&T Bell Laboratories.

by operating at a Bit Error Rate (BER) less than 10^{-5}, we obtain so-called toll-quality speech.[2] For channels where the BER significantly exceeds 10^{-5}, for example, radio channels, the distortion in the recovered speech due to transmission errors becomes significant, dominating the encoder noise. The distortion due to transmission errors is known as digital noise,[3,4] and can be combatted by means of channel coding,[5,6] weighting the amplitude of the binary bits prior to transmission,[7-9] or by post-enhancement procedures.[10-12]

In this study we are concerned with determining the digital noise power in μ-law PCM radio transmission systems. We examine this power for different radio channels, methods of Radio Frequency (RF) modulation, types of binary encoding, bit scrambling, and the application of diversity. In Section II we quantify digital noise power, while in Section III we state our objective performance criterion. We examine two types of channels, the Gaussian in Section IV, and the Rayleigh fading channel in Section V. In the latter case we investigate the effect of scrambling the μ-law PCM bit stream prior to transmission, and the advantages of diversity. The modulation methods considered are Noncoherent Frequency Shift Keying (NCFSK) and Coherent Phase Shift Keying (CFSK). The minimum distance code designed for low-level speech is described in Section VI. In Section VII we discuss the performance of the various μ-law PCM radio systems, where our theoretical formulae are presented in graphical formats, along with simulation results for speech signals, and show the experimental results for μ-law PCM speech transmitted over a mobile radio channel. In the last section we summarize our discourse and draw conclusions.

II. DIGITAL ERRORS IN PCM SYSTEMS

Figure 1 shows a schematic form of the basic companded PCM system. The input sequence $\{x\}$, having a Probability Density Function (PDF) $p_X(x)$, has its amplitude compressed according to the function $f(x)$, and is then uniformly quantized. The combination of the function $f(x)$ and the uniform quantizer produces an effective nonlinear quantizer, as shown in Fig. 2, where $f(x)$ and the number of quantization levels have been selected arbitrarily for the purpose of illustration. The voltage ranges of the input and quantized signals are normalized for convenience to $[-1, 1]$, and the quantized levels are uniformly spaced apart as a result of the uniform quantizer. However, the range of input amplitudes that are quantized to a particular value increases with the magnitude of the input levels. Thus all input amplitudes approximately in the ranges $x_i \pm (\delta_i/2)$ and $x_{i+1} \pm (\delta_{i+1}/2)$ are quantized to y_i and y_{i+1}, respectively, where $\delta_{i+1} > \delta_i$.

Suppose the input signal is sampled at a rate in excess of the

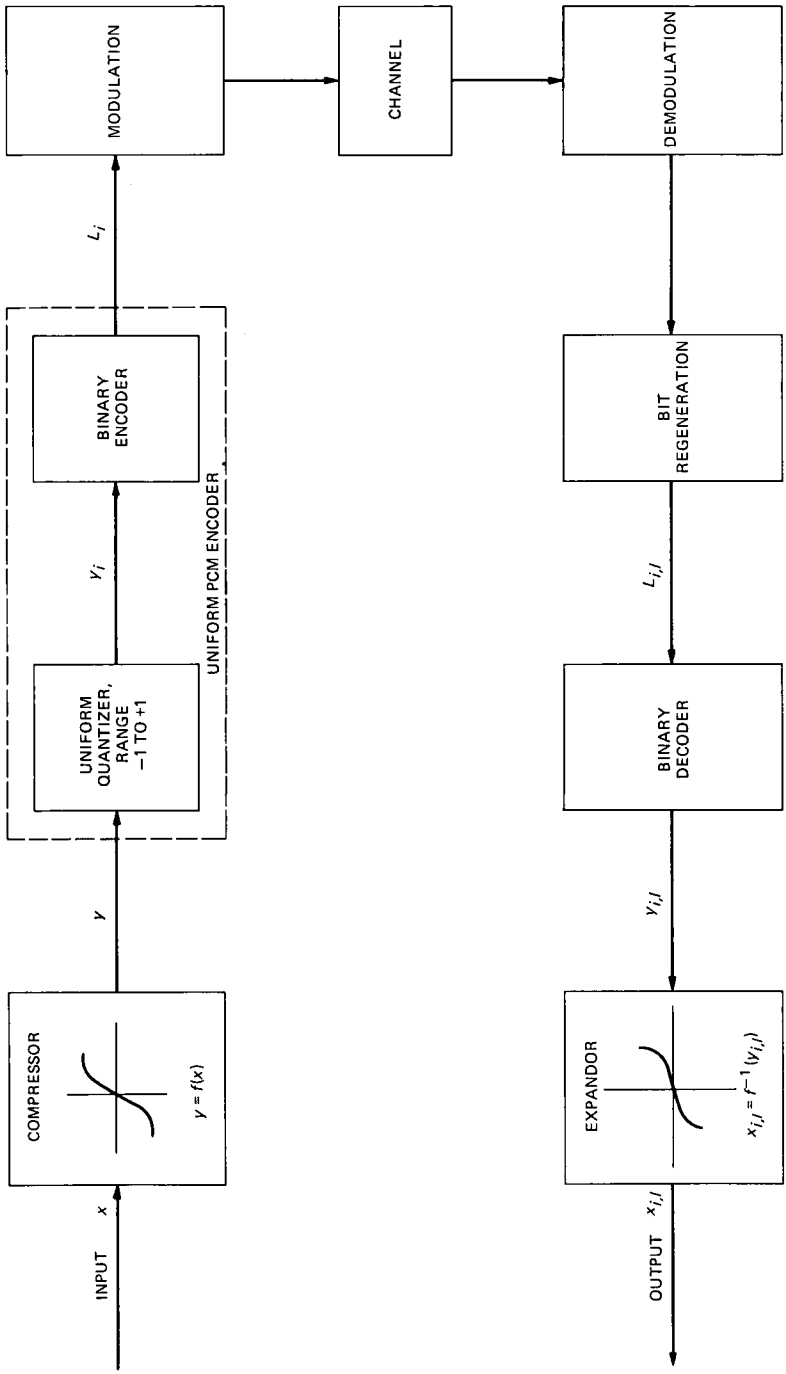

Fig. 1—The basic companded PCM system.

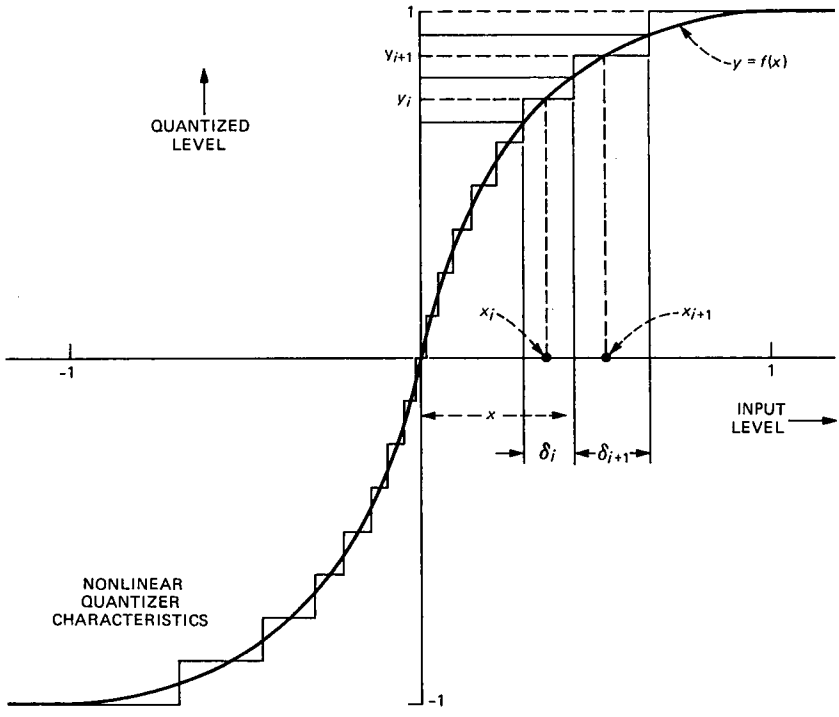

Fig. 2—Exemplary nonlinear quantizer; arbitrary $f(x)$ and number of quantization levels.

Nyquist rate, and the resulting sequence $\{x\}$ is quantized to $\{y\}$. Binary encoding of the quantized sequence ensues to yield $\{L\}$, where each component is an N-bit word. The $\{L\}$ sequence is filtered, modulates a carrier (e.g., using NCFSK), and is transmitted. At the receiver demodulation is performed, and the bits are regenerated. In Fig. 1 we show a particular word L_i at the transmitter, and its regeneration at the receiver as $L_{i,l}$. The word $L_{i,l}$ may be represented by the exclusive-OR ($\oplus$) operation of the binary vectors L_i and e_l,

$$L_{i,l} = L_i \oplus e_l, \tag{1}$$

where $L_{i,l} = L_i$ if no transmission errors occur, and e_l is the lth digital error sequence of length N bits. Whenever the error sequence contains a logical 1 representing the presence of a bit error, the true bit in L_i is inverted, and the error appears in $L_{i,l}$. The N-bit word $L_{i,l}$ is binary decoded to $y_{i,l}$, and the inverse operation of $f(x)$ (i.e., an expansion) is performed to yield the recovered sample,

$$x_{i,l} = f^{-1}(y_{i,l}). \tag{2}$$

The recovered sample $x_{i,l}$ differs from the input sample x, and this

difference is the overall system noise sample. The average noise power in a PCM system is, therefore,

$$\epsilon^2 \triangleq E\{(x - x_{i,l})^2\}, \tag{3}$$

where $E\{(\cdot)\}$ denotes expected value of $(\cdot)$ and is formulated over both source and channel statistics. For the large number of quantization levels considered here, typically 256, the average noise power may be separated into three components, viz:

$$\epsilon^2 = \epsilon_q^2 + \epsilon_c^2 + \epsilon_a^2, \tag{4}$$

where ϵ_q^2, ϵ_c^2, and ϵ_a^2 are the quantization, clipping, and transmission error noise power components, respectively. The noise power generated in the encoder due to the amplitude and time quantization is

$$\epsilon_q^2 + \epsilon_c^2 = E\{(x - x_i)^2\}, \tag{5}$$

where x_i is the recovered sample associated with the quantized sample y_i in the absence of transmission errors, and the expected value is formed over the source statistics. We are more concerned here with the digital noise power, i.e., the noise in the recovered samples due to the presence of digital errors, and we express this power as

$$\epsilon_a^2 = E_{i,l}\{(x_i - x_{i,l})^2\}, \tag{6}$$

where $E_{i,l}(\cdot)$ signifies that the average of $(\cdot)$ is performed over all levels of y_i and all possible error sequences e_l. By observing that the source, e.g., a speech signal and PCM encoder, is independent of the imperfections in the channel, we may express ϵ_a^2 as

$$\epsilon_a^2 = \sum_{l=1}^{2^N-1} \rho_l E_i\{(x_i - x_{i,l})^2\}. \tag{7}$$

The average E_i is formed over all the possible 2^N quantization levels, and ρ_l is the probability of occurrence of the specific error sequence e_l.

At this juncture we introduce the A-factor,[3,4] defined as

$$A_l \triangleq E_i\{(x_i - x_{i,l})^2\}, \tag{8}$$

enabling us to write eq. (7) as

$$\epsilon_a^2 = \sum_{l=1}^{2^N-1} \rho_l A_l. \tag{9}$$

The A-factor A_l is the average noise power at the output of the PCM decoder due to the presence of an error sequence e_l. We have used the notation $e_1, e_2, \cdots, e_N$ to represent the single error bit patterns in the most significant bit (msb), next msb, $\cdots$, least significant bit (lsb), respectively. For example, e_3 is the binary sequence 00100000, implying

the error occurred in the third bit. However, we may have multiple bit errors, and l has integer values that extend to $2^N - 1$, since e_l must contain at least one component that is a logical 1. The number of possible error patterns for w bit errors in an N-bit word is

$$\Omega_w = \binom{N}{w} = \frac{N(N-1)(N-2)\cdots(N-w+1)}{w!}, \tag{10}$$

where the index w is the Hamming weight. When $w = 1$ the N single error bit patterns occur, $w = N$ yields the pattern where every bit in the word is regenerated erroneously, while $\Omega_{N/2}$ is the largest set of error bit patterns. For each error bit pattern there is a unique A-factor, giving $2^N - 1$ different A-factors. For example, the A-factor A_1 applies to a PCM word whose msb bit is erroneously regenerated, and is computed by determining the mean square value of the error $(x_i - x_{i,1})$ over all quantized levels when this particular bit error sequence error is present. The A-factors have a number of attractive properties. They depend only on the source conditions, and not on the channel. Specifically, for the particular number of bits regenerated erroneously in the recovered words and their position in these words, the A-factors depend only on the type of bit allocation, the companding law, and the PDF of x. The A-factors are unaffected by how the bit errors originated. Thus, once we have computed the A-factors for a given source, i.e., input signal and PCM encoder, we can use these factors to calculate the noise due to transmission errors for random channels, fading channels, different modulation schemes, various channel-coding strategies, and so on. Armed with the A-factors we can determine the transmission error power, ϵ_a^2, for any channel that can be characterized by the error sequence probabilities ρ_l, $l = 1$ to $2^N - 1$.

III. PERFORMANCE CRITERION

The objective performance criterion to be used here is the overall signal-to-noise ratio (s/n),

$$\hat{\text{s/n}} = \frac{E\{x^2\}}{\epsilon_q^2 + \epsilon_c^2 + \epsilon_a^2} = \frac{\sigma_x^2}{\epsilon^2} \tag{11}$$

where ϵ^2 is the average noise power [see eq. (4)] and $E\{x^2\}$ or σ_x^2 is the average power of the input sequence. We usually express σ_x^2 in decibels relative to the input level at the start of clipping, i.e., relative to a level magnitude of unity.

IV. THE GAUSSIAN CHANNEL

Consider the situation where the channel errors are independent such that any bit may be in error with probability P. The digital noise

power is given by eq. (9) and can be partitioned into noise power components,

$$\epsilon_a^2 = \epsilon_1^2 + \epsilon_2^2 + \cdots + \epsilon_N^2, \tag{12}$$

where $\epsilon_1^2, \epsilon_2^2, \cdots, \epsilon_N^2$ are the noise powers due to 1-, 2-, $\cdots$, N-bit errors per word, respectively. The first component is

$$\epsilon_1^2 = P_1 \sum_{l=1}^{N} A_l, \tag{13}$$

where P_1 is the probability of a word having a single bit error, namely

$$P_1 = P(1 - P)^{N-1}. \tag{14}$$

The number of A-factors associated with a particular number of bit errors per word depends on N. For example, when $N = 8$, there are 8, 28, 56, 70, 56, 28, 8, and 1 A-factors required in the computation of ϵ_1^2, ϵ_2^2, ϵ_3^2, ϵ_4^2, ϵ_5^2, ϵ_6^2, ϵ_7^2, and ϵ_8^2, respectively. Thus the noise power components of ϵ_a^2 are

$$\epsilon_a^2 = P_1 \sum_{l=1}^{N} A_l + P_2 \sum_{l=N+1}^{N+\binom{N}{2}} A_l + \cdots + P_N A_{2^N-1}, \tag{15}$$

and $P_{(\cdot)}$ is the probability that $(\cdot)$ bits in the N-bit word are regenerated erroneously. Rearranging eq. (15) as

$$\epsilon_a^2 = P_w \sum_{l=l_a+1}^{l_b} A_l;\ w = 1, 2, \cdots, N \tag{16}$$

$$= P_w S_w, \tag{17}$$

where

$$l_a = \sum_{k=0}^{w-1} \binom{N}{k} \tag{18}$$

and

$$l_b = \sum_{k=1}^{w} \binom{N}{k}, \tag{19}$$

and expressing P_w in terms of the average bit error probability P, we have

$$\epsilon_a^2 = P(1 - P)^{N-1} S_1 + P^2(1 - P)^{N-2} S_2 + \cdots + P^N S_N$$

$$= \sum_{w=1}^{N} P^w (1 - P)^{N-w} S_w. \tag{20}$$

From eqs. (16) to (19) we observe that S_w is the sum of the A-factors associated with the Ω_w error sequencies $\{e_l\}$ containing w ones.

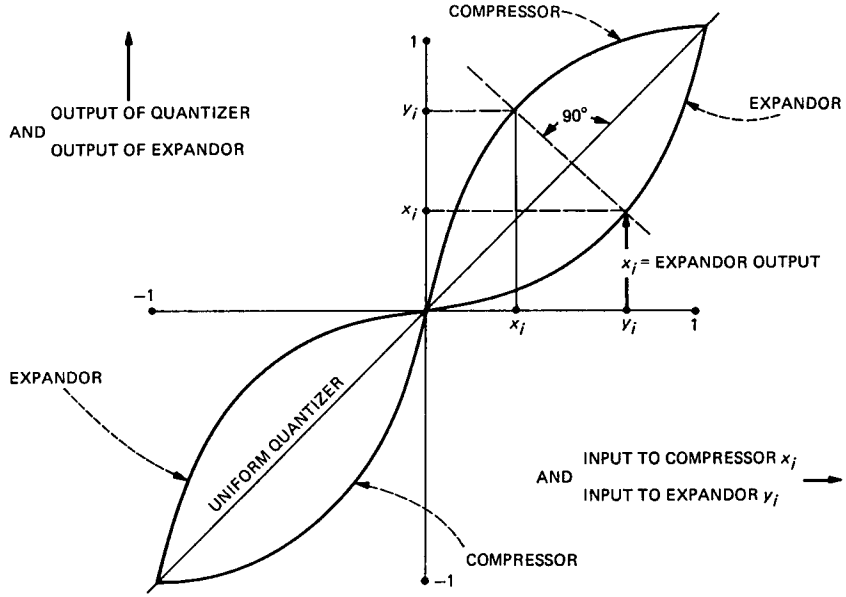

Fig. 3—Compressor and expandor characteristics.

4.1 Determination of the A-factors

Equation (9) shows that the noise power due to transmission errors can be calculated with the aid of a set of A-factors. For the input sequence $\{x\}$ with its PDF $p_X(x)$, the A-factors can be determined using eq. (8), viz:

$$A_l = \sum_{i=0}^{2^N-1} p_X(x_i)\delta_i(x_i - x_{i,l})^2, \tag{21}$$

and the sample x is quantized to y_i if it approximately resides in the range from $x_i - (\delta_i/2)$ to $x_i + (\delta_i/2)$. Figure 3 displays both compressor and expandor characteristics, and we observe that when the quantized level y_i is expanded, the level x_i is recovered. Thus if x falls within δ_i, it is recovered at the receiver as $x_{i,l} = x_i$, assuming no transmission errors occur. If transmission errors are present, the expanded sample at the receiver is $x_{i,l}$. If we assume a large number of quantization levels, the probability density function $p_X(x)$ has an approximately constant value of $p_X(x_i)$ over the interval δ_i. Now the range of the compressor function $f(x)$ is 2, and therefore the N quantized levels are spaced apart by $2/2^N$. Consequently, the slope $f'(x)$ of the compression curve $f(x)$ for an input amplitude x_i is

$$f'(x) = \frac{2^{1-N}}{\delta_i}, \tag{22}$$

and we write eq. (21) as

$$A_l = \sum_{i=0}^{2^N-1} \frac{p_X[f^{-1}(y_i)]2^{1-N}}{f'(f^{-1}(y_i))} [f^{-1}(y_i) - f^{-1}(y_{i,l})]^2 \tag{23}$$

to ease the computation of the A-factors. The values of A_l depend on the PDF of x, the compression characteristic, the bit assignment, and the number and location of the erroneous bits in the PCM word. Thus, we need to determine the A-factors for each PCM system at different input levels.

In this discourse we will perform numerical calculations for the input signal having an exponential PDF,

$$p_X(x) = \frac{1}{\sigma_x \sqrt{2}} \exp\left(-\frac{\sqrt{2}x}{\sigma_x}\right), \tag{24}$$

although our results can be generalized for other PDFs. Unless it is explicitly stated we will assume binary folded PCM is employed, where the msb is the polarity of the quantized sample and the remaining bits represent its magnitude. The PDF $p_X(x)$ of eq. (24) is assumed to be symmetrical about the zero voltage level, and the compandor is an odd function spanning the range from -1 to $+1$.

4.2 Special case of single error A-factors and μ-law companding

To calculate the A-factors for a single bit error in any of the N-bit positions of a PCM word, we express eq. (21) as[6]

$$A_l = \sum_{i=0}^{2^N-1} p_X(x_i)\delta_i a_l(x_i), \tag{25}$$

where

$$a_l(x_i) = (x_i - x_{i,l})^2; \qquad l = 1, 2, \cdots, N, \tag{26}$$

and $l = 1, 2, \cdots, N$ corresponds to a single error in the msb, the next msb, $\cdots$, lsb, respectively. Thus, the $a_l(x_i)$ terms are related to a specific single bit error in the lth bit position, and a specific input signal amplitude x_i. Observe that $a_l(x_i)$ is independent of $p_X(x_i)$, and is a function of the PCM bit code and the compandor rule. By performing the summations in eq. (25) we obtain expressions for the single-error A-factors for a particular PDF $p_X(x_i)$. However, we are concerned here in how the effect of a particular single error varies with x_i, and this we can determine with the aid of the $a_l(x_i)$ functions. Of course, functions of the type of $a_l(x_i)$ can also be derived for any particular multiple-error pattern e_l. The analysis, however, gets increasingly complex.

Before providing a general formula for $a_l(x_i)$, we will consider for

exemplary purposes the case of an error occurring in the second bit position, i.e., $l = 2$. Consider the input sample to have a value x_1, which is compressed to $y_1 = f(x_1)$. Because we are discussing the most significant magnitude bit, an error in this bit will either result in y_1 increasing by 1/2 when a logical 0 is regenerated as a logical 1, or decreasing by a 1/2 when a logical 1 is regenerated as a logical 0. The erroneous decoded y_1 is $f^{-1}[f(x_1) + (1/2)]$ or $f^{-1}[f(x_1) - (1/2)]$, depending on whether the original bit was a logical 0 or 1, respectively. Thus for any x_i we may express $a_2(x_i)$ from eq. (26) as

$$a_2(x_i) = \left[f^{-1}\left[f(x_i) \pm \frac{1}{2}\right] - x_i\right]^2.$$

This method of reasoning enables us to obtain $a_l(x_i)$ for every value of l. For $a_1(x_i)$ we have

$$a_1(x_i) = (2x_i)^2, \qquad 0 \leqslant x_i \leqslant 1, \tag{27}$$

and the general formula for $a_l(x_i)$, $l \geqslant 2$ is

$$a_l(x_i) = \begin{cases} \left\{f^{-1}\left[f(x_i) + \dfrac{1}{2^{(l-1)}}\right] - x_i\right\}^2 & \text{for } f^{-1}\left\{\dfrac{\nu - 1}{2^{(l-1)}}\right\} \\ \quad \leqslant x_i < f^{-1}\left\{\dfrac{\nu}{2^{(l-1)}}\right\}; & \nu \text{ odd} \\ & \nu = 1, 3, \cdots, 2^{(l-1)} - 1 \\ \left\{f^{-1}\left[f(x_i) - \dfrac{1}{2^{(l-1)}}\right] - x_i\right\}^2 & \text{for } f^{-1}\left\{\dfrac{\nu - 1}{2^{(l-1)}}\right\} \\ \quad \leqslant x_i < f^{-1}\left\{\dfrac{\nu}{2^{(l-1)}}\right\}; & \nu \text{ even} \\ & \nu = 2, 4, \cdots, 2^{(l-1)}. \end{cases} \tag{28}$$

So far we have not specified the compression function $f(x_i)$, but as it is our intention to subsequently place considerable emphasis on μ-law PCM we provide now the $a_l(x_i)$ terms for this type of compression. The μ-law compression function is specified by[1]

$$f(x_i) = \frac{\log(1 + \mu x_i)}{\log(1 + \mu)}, \qquad 0 \leqslant x_i \leqslant 1, \tag{29}$$

and the corresponding expansion to recover x_i is

$$x_i = f^{-1}(y_i) = \frac{1}{\mu}\{\exp[y_i \log(1 + \mu)] - 1\}, \qquad 0 \leqslant y_i \leqslant 1. \tag{30}$$

Equation (27) is applicable for μ-law PCM, and the general formula

for $l \geq 2$ is

$$a_l(x_i) = \begin{cases} f^{-1}\left[\dfrac{1}{2^{(l-1)}}\right]^2 (1+\mu x_i)^2 & \text{for } f^{-1}\left\{\dfrac{\nu-1}{2^{(l-1)}}\right\} \\ \quad \leq x_i < f^{-1}\left\{\dfrac{\nu}{2^{(l-1)}}\right\}; & \nu \text{ odd} \\ & \nu = 1, 3, \cdots, 2^{(l-1)} - 1 \\ (1+\mu)^{-\frac{1}{2^{(l-2)}}} \cdot f^{-1}\left[\dfrac{1}{2^{(l-1)}}\right]^2 (1+\mu x_i)^2 & \text{for } f^{-1}\left\{\dfrac{\nu-1}{2^{(l-1)}}\right\} \\ \quad \leq x_i < f^{-1}\left\{\dfrac{\nu}{2^{(l-1)}}\right\}; & \nu \text{ even} \\ & \nu = 2, 4, \cdots, 2^{(l-1)}. \end{cases} \tag{31}$$

Inserting $a_l(x_i)$ and $p_X(x_i)$ from eqs. (27), (31), and (24), respectively, into eq. (25) enables us to compute the single bit error A-factors for μ-law PCM.

The variation of the $a_l(x_i)$ factors as a function of quantized level x_i, $l = 1, 2, \cdots, 8$, is displayed in Fig. 4 for 8-bit μ-law PCM, $\mu = 255$. As we expected from eq. (27), where $l = 1$, $a_1(x_i)$ is a monotonic function as shown in Fig. 4a. Let us consider the case of $l = 2$ when the single error occurs in the magnitude bit. To provide some insight into $a_2(x_i)$, we note that its value in eq. (28) is

$$a_2(x_i) = \begin{cases} f^{-1}\left[f(x_i) + \dfrac{1}{2}\right] - x_i\Big\}^2; & 0 \leq x_i < f^{-1}\left(\dfrac{1}{2}\right) \\ f^{-1}\left[f(x_i) - \dfrac{1}{2}\right] - x_i\Big\}^2; & f^{-1}\left(\dfrac{1}{2}\right) \leq x_i \leq 1. \end{cases} \tag{32}$$

If we substitute $f(x_i)$ into $a_2(x_i)$, and for the moment confine ourselves to $0 \leq x_i < f^{-1}(1/2)$, we have

$$a_2(x_i) = \left\{f^{-1}\left[\frac{\log(1+\mu x_i)}{\log(1+\mu)} + \frac{1}{2}\right] - x_i\right\}^2, \tag{33}$$

and on applying eq. (30)

$$\begin{aligned} a_2(x_i) &= \left(\frac{1}{\mu}\left\{\exp[\log(1+\mu x_i) + \frac{1}{2}\log(1+\mu)] - 1\right\} - x_i\right)^2 \\ &= \left[\frac{1}{\mu}\left(\sqrt{1+\mu} - 1\right)\right]^2 (1+\mu x_i)^2. \end{aligned} \tag{34}$$

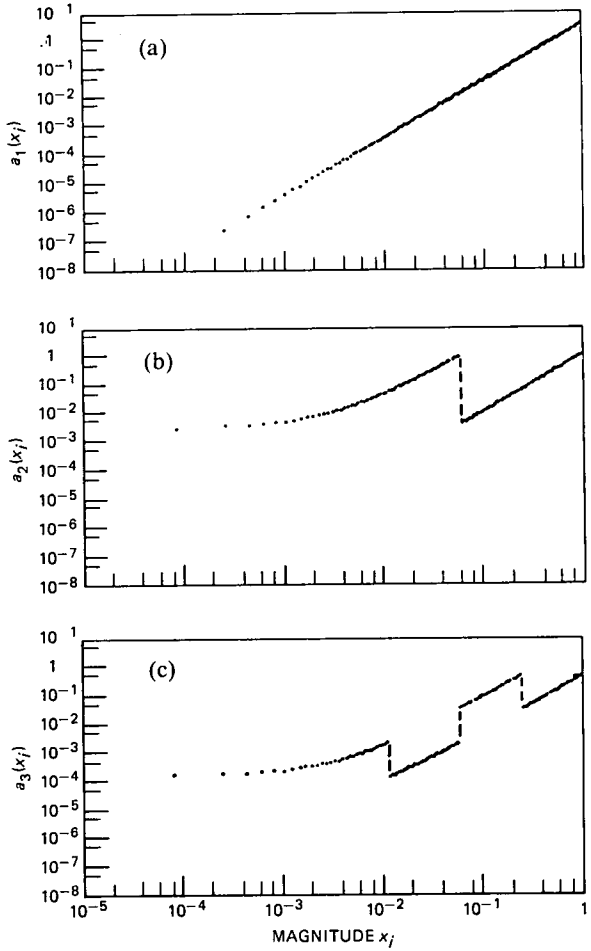

Fig. 4—Variation of $a_l(x_i)$ as a function of x_i for 8-bit μ-law PCM, $\mu = 255$. The subfigures a through h apply for a single bit error in the msb ($l = 1$), the next msb ($l = 2$), $\cdots$, lsb ($l = 8$), respectively.

From eq. (30) the value of x_i when $y_i = 1/2$ is

$$f^{-1}\left(\frac{1}{2}\right) = \frac{1}{\mu}\left[e^{[1/2]\log(1+\mu)} - 1\right]$$

$$= \frac{1}{\mu}\left(\sqrt{1+\mu} - 1\right), \tag{35}$$

and hence we obtain

$$a_2(x_i) = \left[f^{-1}\left(\frac{1}{2}\right)\right]^2 (1 + \mu x_i)^2; \qquad 0 \leq x_i < f^{-1}\left(\frac{1}{2}\right), \tag{36}$$

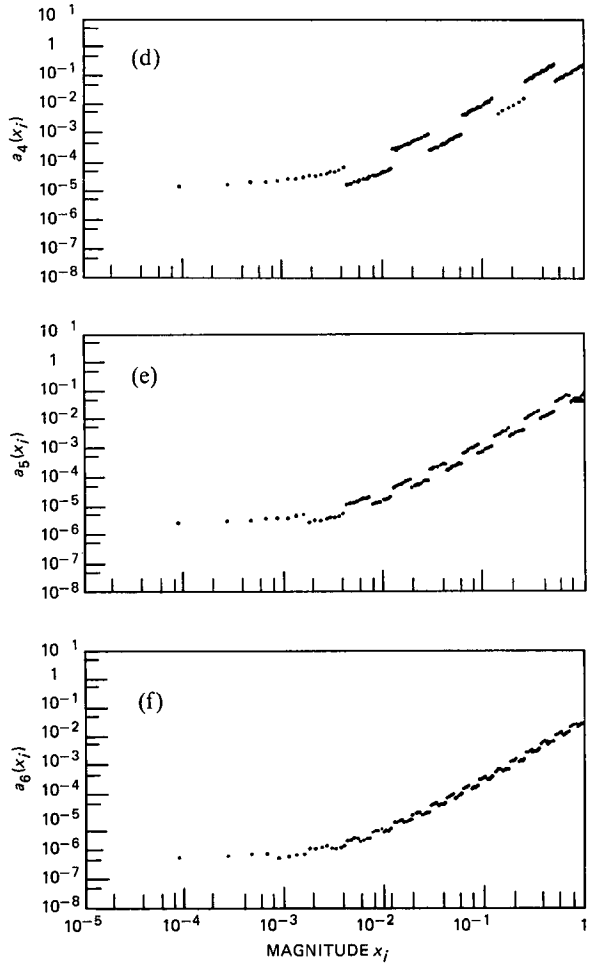

Fig. 4—Continued.

the value given by eq. (31). Observe that $y_i = 1/2$ marks the boundary between the most significant magnitude bit being 0 ($y_i < 1/2$), and being a logical 1 ($y_i \geq 1/2$). Consequently, an error in the most significant magnitude bit changes the magnitude of the quantized signal by a 1/2. However, the change in $x_{i,l}$ is not a 1/2, being dependent on the μ-law. Figure 5 illustrates that if the input sample has a small amplitude, x_1 say, and is compressed to y_1, then the effect of an error in the most significant magnitude bit is to cause y_1 to increase by half the range to $y_{1,l}$. The corresponding decoded signal is $x_{1,l}$, having an error E_1 of $\sqrt{a_2(x_1)}$. If the input sample amplitude is larger, say x_2, and the same bit is inverted, $x_{2,l}$ is recovered having an error E_2 of

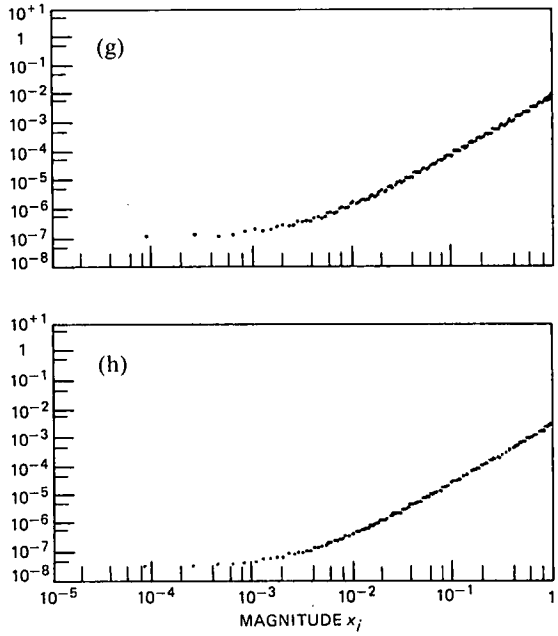

Fig. 4—Continued.

$\sqrt{a_2(x_2)}$ that is significantly larger than E_1. Thus the errors become significantly larger as y_i moves closer to 1/2. The variation of $a_2(x_i)$ over the range of x from zero to f^{-1} (1/2) is shown in Fig. 4b. As we expected from eq. (36), when x_i is very small, $a_2(x_i)$ is a constant equal to $[f^{-1}(1/2)]^2$. As x_i approaches $f^{-1}(1/2)$,

$$a_2(x_i) \simeq [f^{-1}(1/2)]^2 \mu^2 x_i^2 \tag{37}$$

and the variation appears as a straight line in the figure.

Consider the situation when x_i exceeds $f^{-1}(1/2)$. An input x_3 (see Fig. 5), encoded to y_3 and then subjected to an error in the second bit position, is reduced to $x_{3,l}$, and the resulting error E_3 of $\sqrt{a_2(x_3)}$ is less than E_2 and of opposite polarity. We therefore observe in Fig. 4b a discontinuity in $a_2(x_i)$ as x_i just exceeds $f^{-1}(1/2)$, causing it to plummet. By applying similar arguments to those employed in establishing eq. (36), we obtain the result given in eq. (31), namely,

$$a_2(x_i) = \frac{\left[f^{-1}\left(\frac{1}{2}\right)\right]^2}{1+\mu}(1+\mu x_i)^2; \qquad f^{-1}\left(\frac{1}{2}\right) \leqslant x_i \leqslant 1. \tag{38}$$

When $\mu x \gg 1$, $a_2(x_i)$ is proportional to x_i^2, as can be seen in Fig. 4b for $x_i \geqslant f^{-1}$ (1/2).

When errors occur in the third msb, i.e., $l = 3$, we have from eq. (31),

$$a_3(x_i) = \begin{cases} \left[f^{-1}\left(\frac{1}{4}\right)\right]^2 (1 + \mu x_i)^2; & 0 \leq x_i < f^{-1}\left(\frac{1}{4}\right) \\ \dfrac{\left[f^{-1}\left(\frac{1}{4}\right)\right]^2}{\sqrt{1+\mu}} (1 + \mu x_i)^2; & f^{-1}\left(\frac{1}{4}\right) \leq x_i < f^{-1}\left(\frac{1}{2}\right) \\ \left[f^{-1}\left(\frac{1}{4}\right)\right]^2 (1 + \mu x_i)^2; & f^{-1}\left(\frac{1}{2}\right) \leq x_i < f^{-1}\left(\frac{3}{4}\right) \\ \dfrac{\left[f^{-1}\left(\frac{1}{4}\right)\right]^2}{\sqrt{1+\mu}} (1 + \mu x_i)^2; & f^{-1}\left(\frac{3}{4}\right) \leq x_i \leq f^{-1}(1). \end{cases} \tag{39}$$

From this equation the variation of $a_3(x_i)$ with x_i is evident. The abrupt changes occur at $f^{-1}(1/4)$, $f^{-1}(1/2)$, and $f^{-1}(3/4)$, because the transmission errors cause y_i to change by 1/4. Thus the detailed discussion relating to $a_2(x_i)$ and Fig. 5 are relevant here, but instead of one transition at $f^{-1}(1/2)$ there are three logical transitions for this case of $l = 3$.

For higher values of l there are more transitions in y_i due to transmission errors, and these manifest as more discontinuities in $a_l(x_i)$. For $l = 8$ the logical value of the lsb changes with each succeeding x_i, and as a consequence there are 128 discontinuities in $a_8(x_i)$, although the magnitude of the jumps in $a_8(x_i)$ at the discontinuities are miniscule. The result is that the curve of $a_8(x_i)$, shown in Fig. 4h, appears to be almost smooth.

4.3 Computing the overall s/n

The digital noise power ϵ_a^2 is dependent on the type of digital modulation. For noncoherent frequency shift keying (NCFSK) the bit error probability is[13]

$$P = \frac{1}{2} e^{-\frac{E}{2N_o}}, \tag{40}$$

where E is the bit energy and N_o is the one-sided spectral density function of the white Gaussian noise in the channel. When coherent phase shift keying (CPSK) is employed, the bit error probability is

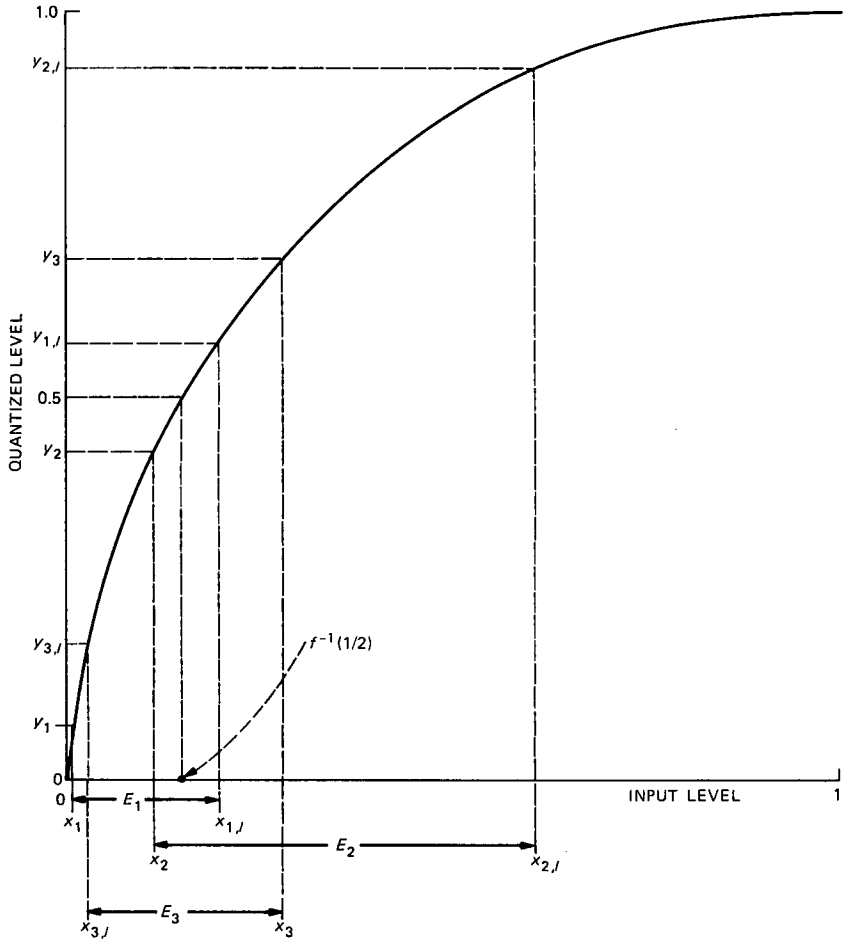

Fig. 5—The nonlinear quantizer characteristic showing how the effect of a transmission error in the second msb ($l = 2$) affects the amplitude of the recovered sample.

given by[13]

$$P = Q\left(\sqrt{\frac{2E}{N_o}}\right). \tag{41}$$

When the values of P given by eq. (40) or eq. (41) are substituted into eq. (20), the digital noise power for NCFSK and CPSK are determined. The knowledge of ϵ_a^2 enables $\hat{s/n}$ to be determined using eq. (11).

V. RAYLEIGH FADING CHANNELS

In Section IV we provide an expression [see eq. (20)] that enables us to calculate the noise power in the recovered signal due to trans-

mission errors in μ-law PCM. The bit errors are considered to be statistically independent. We now turn our attention to transmission channels that contain both additive Gaussian noise and Rayleigh signal fading. Our investigation considers both the effects of scrambling (also called interleaving) and not scrambling the bits prior to transmission, as well as the application of diversity techniques to reduce the digital noise power. We commence by considering the case of NCFSK modulation.

5.1 Digital noise power with NCFSK modulation

5.1.1 Bit scrambling prior to transmission

If the bit stream is scrambled prior to its transmission over a Rayleigh fading channel, and the regenerated bit stream is descrambled at the receiver, then the bit errors will tend to be statistically independent. By the process of scrambling, the burst errors that occur in Rayleigh fading environments are randomized. Because the transmitted signal is subjected to Rayleigh fading, the channel s/n γ is a random variable having a PDF of[13]

$$f(\gamma) = \frac{1}{\Gamma} e^{-\gamma/\Gamma}, \tag{42}$$

where Γ is the average bit signal-to-noise ratio, viz:

$$\Gamma = E\{\gamma\}. \tag{43}$$

The average bit error probability for the Rayleigh fading channel with its additive Gaussian noise is[13]

$$P_F = \int_o^\infty f(\gamma)P(\gamma)d\gamma, \tag{44}$$

where

$$P(\gamma) = \frac{1}{2} e^{-\gamma/2}, \tag{45}$$

resulting in

$$P_F = \frac{1}{2 + \Gamma}. \tag{46}$$

Substituting P_F from eq. (46) as P into eq. (20) yields the digital noise power for bit scrambling, NCFSK, and a Rayleigh fading channel, viz:

$$\epsilon^2_{a,F,S} = \sum_{w=1}^{N} \left(\frac{1}{2 + \Gamma}\right)^w \left(1 - \frac{1}{2 + \Gamma}\right)^{N-w} S_w,$$

or $\epsilon^2_{a,F,S}$ may be expressed as

$$\epsilon^2_{a,F,S} = \sum_{w=1}^{N} \frac{T_w}{(2 + \Gamma)^w} = \sum_{w=1}^{N} P_F^w T_w, \tag{47}$$

where the subscripts F and S signify a fading channel and the application of bit scrambling, respectively. The term T_w is

$$T_w = \sum_{j=1}^{w} S_w \binom{N-j}{w-j} (-1)^{w-j}; \qquad w = 1, 2, \cdots, N, \tag{48}$$

and S_w can be determined from eqs. (16) through (19). For $P_F \ll 1$, the only value of w that need be considered is 1, and hence

$$\epsilon_a^2 = \frac{T_1}{2 + \Gamma} = \frac{S_1}{2 + \Gamma}. \tag{49}$$

5.1.2 No bit scrambling prior to transmission

We assume that the fading is sufficiently slow for γ to be constant over an N-bit period, i.e., over the duration of one PCM word. The probability of w bits being erroneously regenerated for a particular value of γ is $P(\gamma)^w[1 - P(\gamma)]^{N-w}$. When the bits are not scrambled the average probability of w bits being regenerated erroneously is

$$P_{w,F,\bar{S}} = \int_0^\infty P(\gamma)^w[1 - P(\gamma)]^{N-w} f(\gamma)d\gamma, \tag{50}$$

where the subscripts w, F, $\bar{S}$, signify w bits in error, a fading situation, and no bit scrambling, respectively. Applying a similar procedure to that used in establishing eq. (20) enables us to determine the digital noise power for the Rayleigh fading channel when no bit scrambling is employed, viz:

$$\begin{aligned}\epsilon_{a,F,\bar{S}} &= S_1 \int_0^\infty P(\gamma)[1 - P(\gamma)]^{N-1} f(\gamma)d\gamma \\ &\quad + S_2 \int_0^\infty P(\gamma)^2[1 - P(\gamma)]^{N-2} f(\gamma)d\gamma \\ &\quad + \cdots + S_8 \int_0^\infty P(\gamma)^N f(\gamma)d\gamma \\ &= \sum_{w=1}^{N} P_{w,F,\bar{S}} S_w. \end{aligned} \tag{51}$$

An alternative representation is

$$\epsilon^2_{a,F,\bar{S}} = \sum_{w=1}^{N} T_w \int_o^\infty f(\gamma) P^w(\gamma)d\gamma, \tag{52}$$

where T_w is given by eq. (48). The integral expression in eq. (52) is, from eqs. (42) and (45),

$$\int_o^\infty f(\gamma)P^w(\gamma)d\gamma = \frac{1}{2^{w-1}(2 + \Gamma w)}, \tag{53}$$

and consequently the digital noise power for a slow fading channel and no bit scrambling is

$$\epsilon^2_{a,F,\bar{S}} = \sum_{w=1}^{N} \frac{T_w}{2^{w-1}(2 + \Gamma w)}. \tag{54}$$

5.1.3 *Effect of diversity*

The average digital noise power formulae will now be derived when diversity is applied, where the type of diversity, e.g., space, frequency, time, polarization, is immaterial. For M-fold diversity reception with ideal maximal-ratio combining, the PDF of the channel s/n γ is[13]

$$f(\gamma) = \frac{\gamma^{M-1}e^{-\gamma/\Gamma}}{\Gamma^M(M-1)!}. \tag{55}$$

If the receiver selects the diversity branch having the strongest signal level the diversity scheme is known as ideal selection combining for which the PDF is[13]

$$f(\gamma) = \frac{M}{\Gamma} e^{-\gamma/\Gamma}(1 - e^{-\gamma/\Gamma})^{(M-1)}. \tag{56}$$

5.1.3.1 Bit scrambling employed. Substituting $f(\gamma)$ from eq. (55) and $P(\gamma)$ from eq. (45) into eq. (44) gives the average bit error probability. When this probability is substituted in eq. (47) the digital noise for the ideal maximal-ratio combining becomes

$$\epsilon^2_{a,F,S,D} = \sum_{w=1}^{N} T_w \left[\frac{2^{M-1}}{(2 + \Gamma)^M}\right]^w, \tag{57}$$

where the subscript D signifies the application of diversity reception.

When the process is repeated using $f(\gamma)$ from eq. (56), the digital noise power for ideal selection combining is obtained, viz:

$$\epsilon^2_{a,F,S,D} = \left[\sum_{w=1}^{N} T_w \quad \frac{M}{2\Gamma} \sum_{j=0}^{M-1} (-1)^j \binom{M-1}{j} \frac{1}{\left(\frac{1}{\Gamma} + \frac{j}{\Gamma} + \frac{1}{2}\right)}\right]^w. \tag{58}$$

5.1.3.2 No bit scrambling prior to transmission. When ideal maximal-ratio combining is employed, application of eqs. (45) and (55) yields

$$\int_o^\infty P^w(\gamma)f(\gamma)d\gamma = \frac{2^{M-w}}{(2 + \Gamma w)^M} \tag{59}$$

for NCFSK modulation. The digital noise power is then determined to be

$$\epsilon^2_{a,F,\bar{S},D} = \sum_{w=1}^{N} T_w \frac{2^{M-w}}{(2 + \Gamma w)^M}. \tag{60}$$

For ideal selection combining the expression

$$\int_o^\infty P^w(\gamma) f(\gamma) d\gamma = \frac{M}{\Gamma 2^w} \sum_{j=0}^{M-1} (-1)^j \binom{M-1}{j} \frac{1}{\left(\frac{1}{\Gamma} + \frac{j}{\Gamma} + \frac{w}{2}\right)} \tag{61}$$

is established by means of eqs. (45) and (56) and the application of the technique described in Ref. 14. The digital noise power for the situation described here is

$$\epsilon^2_{a,F,\bar{S},D} = \sum_{w=1}^{N} \frac{MT_w}{\Gamma 2^w} \sum_{j=0}^{M-1} (-1)^j \binom{M-1}{j} \frac{1}{\left(\frac{1}{\Gamma} + \frac{j}{\Gamma} + \frac{w}{2}\right)}. \tag{62}$$

5.2 Digital noise power with CPSK modulation

The differences in the digital noise power of the PCM system using CPSK and NCFSK modulation are due to the differences of their probability of bit error. For CPSK the probability of bit error as a function of channel s/n is[15]

$$P(\gamma) = Q(\sqrt{2\gamma}). \tag{63}$$

The distribution functions for the channel s/n's are given by eqs. (55) and (56) for the case of maximal-ratio-combining diversity and ideal selection-combining diversity, respectively. When bit scrambling is performed prior to transmission, the average bit error probability is computed using eq. (44), where $P(\gamma)$ is given by eq. (63), and $f(\gamma)$ is selected from either eq. (55) or (56). This average bit error probability is substituted into eq. (47) to give the digital noise power, from which, with the aid of eq. (11) $\hat{s/n}$ is formulated.

When the bits are not scrambled, the digital noise power is found by substituting $P(\gamma)$ from eq. (63), and $f(\gamma)$ from either eq. (55) or (56) directly into eq. (52). With the aid of eqs. (52) and (11), $\hat{s/n}$ is determined.

VI. MINIMUM DISTANCE CODE PCM

The folded binary PCM code has its msb as the polarity of the encoded sample, while the remaining bits constitute the magnitude of the sample. In natural binary code the most negative sample is given an all-zero pattern, and binary numbering of progressively more pos-

itive samples ensues until the most positive sample is reached, which is assigned an all-one code. A single error in these codes can produce large errors in the recovered samples. The Gray code is also vulnerable to transmission errors, although the magnitude of the errors is not as large as those encountered when the folded binary and natural binary codes are employed.

The Minimum Distance Code (MDC) was conceived by Rydbeck and Sundberg.[3] The word distance in this code name refers to the difference between a recovered sample correctly received and its value when subjected to a single bit error. The MDC has the property of asymptotic minimum digital noise for low-level speech samples, and the abbreviation may also be taken as minimum digital noise code. The structure of the code is based on the error sequencies discussed in Section II. The msb represents the polarity of the quantized sample, being logical 0 for positive samples and logical 1 for negative samples. Table I shows the seven-bit magnitude code for 8-bit PCM. For quantized level number y_i of zero we have an all-zero word. The code words for $y_i = 1$ to 7 are the single error patterns when the Hamming weight w is unity. The next group is the double error ($w = 2$) patterns having 21 components extending from $y_i = 8$ to 28 inclusive. The code progresses, having 35 triple-error sequencies, $w = 3$, and so on until the final all logical 1 code when $w = 7$. The number code words in each group represented by the Hamming weight w are

$$\binom{N-1}{w}.$$

The MDC code is specifically designed to accommodate low-level input signals. When single bit errors occur the code can only change to an adjacent group. Changes involving half the magnitude range that occurs in folded binary PCM are forbidden. However, errors in the least significant bits will in general cause much larger errors in the recovered sample than in folded binary. We therefore trade the large erroneous spikes in the recovered signal that occur in folded binary PCM for smaller spikes that happen more frequently in MDC.

VII. PERFORMANCE

The input range of the quantizer was from -1 to $+1$, and in our theoretical calculations the input signal was assumed to have an exponential PDF with standard deviation of either $\sqrt{2}/10$ (-17 dB), or 0.01 (-40 dB). The 8-bit μ-law PCM encoder, $\mu = 255$, was arranged to operate at input signal powers of -17 dB and -40 dB, the former being indicative of high-level speech and the latter of low-level speech. Three binary codes were considered initially—Natural Binary Code

Table I—The MDC code for 8-bit PCM (the polarity bit is not shown)

Quantized Level Number	Magnitude Code of MDC							w
127	1	1	1	1	1	1	1	7
126	1	1	1	1	1	1	0	6
125	1	1	1	1	1	0	1	6
124	1	1	1	1	0	1	1	6
123	1	1	1	0	1	1	1	6
122	1	1	0	1	1	1	1	6
121	1	0	1	1	1	1	1	6
120	0	1	1	1	1	1	1	6
119	1	1	1	1	1	0	0	5
118	1	1	1	1	0	1	0	5
117	1	1	1	0	1	1	0	5
116	1	1	0	1	1	1	0	5
115	1	0	1	1	1	1	0	5
114	0	1	1	1	1	1	0	5
113	1	1	1	1	0	0	1	5
112	1	1	1	0	1	0	1	5
111	1	1	0	1	1	0	1	5
110	1	0	1	1	1	0	1	5
109	0	1	1	1	1	0	1	5
108	1	1	1	0	0	1	1	5
107	1	1	0	1	0	1	1	5
106	1	0	1	1	0	1	1	5
105	0	1	1	1	0	1	1	5
104	1	1	0	0	1	1	1	5
103	1	0	1	0	1	1	1	5
102	0	1	1	0	1	1	1	5
101	1	0	0	1	1	1	1	5
100	0	1	0	1	1	1	1	5
99	0	0	1	1	1	1	1	5
98	1	1	1	1	0	0	0	4
97	1	1	1	0	1	0	0	4
96	1	1	0	1	1	0	0	4
95	1	0	1	1	1	0	0	4
94	0	1	1	1	1	0	0	4
93	1	1	1	0	0	1	0	4
92	1	1	0	1	0	1	0	4
91	1	0	1	1	0	1	0	4
90	0	1	1	1	0	1	0	4
89	1	1	0	0	1	1	0	4
88	1	0	1	0	1	1	0	4
87	0	1	1	0	1	1	0	4
86	1	0	0	1	1	1	0	4
85	0	1	0	1	1	1	0	4
84	0	0	1	1	1	1	0	4
83	1	1	1	0	0	0	1	4
82	1	1	0	1	0	0	1	4
81	1	0	1	1	0	0	1	4
80	0	1	1	1	0	0	1	4
79	1	1	0	0	1	0	1	4
78	1	0	1	0	1	0	1	4
77	0	1	1	0	1	0	1	4
76	1	0	0	1	1	0	1	4
75	0	1	0	1	1	0	1	4
74	0	0	1	1	1	0	1	4
73	1	1	0	0	0	1	1	4
72	1	0	1	0	0	1	1	4
71	0	1	1	0	0	1	1	4

Quantized Level Number	Magnitude Code of MDC							w
70	1	0	0	1	0	1	1	4
69	0	1	0	1	0	1	1	4
68	0	0	1	1	0	1	1	4
67	1	0	0	0	1	1	1	4
66	0	1	0	0	1	1	1	4
65	0	0	1	0	1	1	1	4
64	0	0	0	1	1	1	1	4
63	1	1	1	0	0	0	0	3
62	1	1	0	1	0	0	0	3
61	1	0	1	1	0	0	0	3
60	0	1	1	1	0	0	0	3
59	1	1	0	0	1	0	0	3
58	1	0	1	0	1	0	0	3
57	0	1	1	0	1	0	0	3
56	1	0	0	1	1	0	0	3
55	0	1	0	1	1	0	0	3
54	0	0	1	1	1	0	0	3
53	1	1	0	0	0	1	0	3
52	1	0	1	0	0	1	0	3
51	0	1	1	0	0	1	0	3
50	1	0	0	1	0	1	0	3
49	0	1	0	1	0	1	0	3
48	0	0	1	1	0	1	0	3
47	1	0	0	0	1	1	0	3
46	0	1	0	0	1	1	0	3
45	0	0	1	0	1	1	0	3
44	0	0	0	1	1	1	0	3
43	1	1	0	0	0	0	1	3
42	1	0	1	0	0	0	1	3
41	0	1	1	0	0	0	1	3
40	1	0	0	1	0	0	1	3
39	0	1	0	1	0	0	1	3
38	0	0	1	1	0	0	1	3
37	1	0	0	0	1	0	1	3
36	0	1	0	0	1	0	1	3
35	0	0	1	0	1	0	1	3
34	0	0	0	1	1	0	1	3
33	1	0	0	0	0	1	1	3
32	0	1	0	0	0	1	1	3
31	0	0	1	0	0	1	1	3
30	0	0	0	1	0	1	1	3
29	0	0	0	0	1	1	1	3
28	1	1	0	0	0	0	0	2
27	1	0	1	0	0	0	0	2
26	0	1	1	0	0	0	0	2
25	1	0	0	1	0	0	0	2
24	0	1	0	1	0	0	0	2
23	0	0	1	1	0	0	0	2
22	1	0	0	0	1	0	0	2
21	0	1	0	0	1	0	0	2
20	0	0	1	0	1	0	0	2
19	0	0	0	1	1	0	0	2
18	1	0	0	0	0	1	0	2
17	0	1	0	0	0	1	0	2
16	0	0	1	0	0	1	0	2
15	0	0	0	1	0	1	0	2

Table I—*Continued*

Quantized Level Number	Magnitude Code of MDC							w	Quantized Level Number	Magnitude Code of MDC							w
14	0	0	0	0	1	1	0	2	6	0	1	0	0	0	0	0	1
13	1	0	0	0	0	0	1	2	5	0	0	1	0	0	0	0	1
12	0	1	0	0	0	0	1	2	4	0	0	0	1	0	0	0	1
11	0	0	1	0	0	0	1	2	3	0	0	0	0	1	0	0	1
10	0	0	0	1	0	0	1	2	2	0	0	0	0	0	1	0	1
9	0	0	0	0	1	0	1	2	1	0	0	0	0	0	0	1	1
8	0	0	0	0	0	1	1	2	0	0	0	0	0	0	0	0	0
7	1	0	0	0	0	0	0	1									

(NBC), Folded Binary Code (FBC), and Minimum Distance Code (MDC)—but it soon transpired that NBC was considerably inferior to the others and was abandoned. In Table II we display the single-error A-factors and the T-factors of eqs. (25) and (48), respectively. The input signal has an exponential PDF specified by eq. (24), and the codec is 8-bit μ-law PCM, $\mu = 255$. The factors $A_1, A_2, \cdots, A_8$ are associated with single errors in the first, second, $\cdots$, lsb, respectively. The entries in the table illustrate that the variation between the A-factors is significantly smaller for MDC than for FBC. Consequently, the digital noise power due to single bit errors per word when the MDC code is used is similar for all bit locations in the words. This situation is radically different when FBC is employed. For low-level speech the factor T_1 for MDC is significantly smaller than its counterpart with FBC. When the input level is high, the T_1 factors are approximately the same. Unlike the case of linear PCM with FBC, where T_3 to T_8 are zero,[16] the T-factors with companded PCM are nonzero.

The types of modulation employed in our analysis were NCFSK and CPSK. The quantization noise power ϵ_q^2 and clipping noise power ϵ_c^2 were determined for the input powers of -17 and -40 dB in the absence of transmission errors. The digital noise power ϵ_a^2 was computed using the equations in Sections IV and V. Armed with knowledge of these noise powers we were able to compute the theoretical overall s/n, namely $\widehat{s/n}$, as expressed by eq. (11). As ϵ_a^2 is a function of channel s/n, the variation of $\widehat{s/n}$ with channel s/n was determined.

In addition to presenting these theoretical variations of $\widehat{s/n}$, we also conducted simulations using speech signals. In our experiments we used four concatenated sentences: "Glue the sheet to the dark blue background," "Rice is often served in round bowls," "Four hours of steady work faced us," and "The box was thrown beside the parked truck." The first two sentences were spoken by females, the others by males. The speech was bandlimited between 200 and 3200 Hz, and sampled at 8 kHz to give the speech sequence used in our simulations.

Table II—The single error A- and T-factors for 8-bit μ-law PCM, $\mu = 255$; the input PDF is exponential

	A_1	A_2	A_3	A_4	A_5	A_6	A_7	A_8
−40 dB/FBC	3.954e-4	3.783e-2	6.375e-4	1.105e-4	2.184e-5	5.176e-6	1.277e-6	3.181e-7
−40 dB/MDC	3.954e-4	2.486e-3	2.220e-3	1.982e-3	1.632e-3	1.161e-3	5.833e-4	1.389e-4
−17 dB/FBC	0.07906	0.1391	0.08739	0.01331	2.644e-3	6.281e-4	1.550e-4	3.863e-5
−17 dB/MDC	0.07906	0.05214	0.04879	0.04554	0.04118	0.3434	0.02405	0.01009
	T_1	T_2	T_3	T_4	T_5	T_6	T_7	T_8
−40 dB/FBC	0.03900	0.2871	4.914e-3	−4.108e-2	2.155e-4	6.056e-5	3.576e-7	−1.788e-7
−40 dB/MDC	0.01060	0.3019	0.3811	−1.024	0.9891	−0.4009	0.03743	−4.965e-3
−17 dB/FBC	0.3223	−0.1182	−0.2133	0.06660	0.003221	−1.976e-4	2.980e-7	−1.192e-7
−17 dB/MDC	0.3352	−0.06155	−0.7784	1.480	−1.660	1.052	−0.4118	0.1041

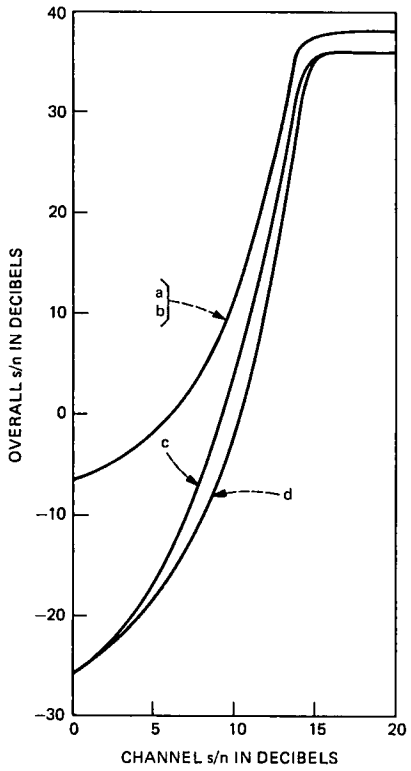

Fig. 6—Gaussian channel. Theoretical curves of overall s/n against channel s/n for NCFSK modulation (a) −17 dB input power, MDC; (b) −17 dB input power, FBC; (c) −40 dB input power, MDC; and (d) −40 dB input power, FBC.

7.1 Gaussian channel

The theoretical curves of $\hat{s}/n$ versus channel s/n when NCFSK modulation was employed are displayed in Fig. 6. When the input signal power was −17 dB there was negligible difference between the curves corresponding to FBC and MDC binary codes. Reducing the input signal power to −40 dB revealed differences in the two codes, with MDC producing a gain in $\hat{s}/n$ compared to FBC of up to 4 dB for a given channel s/n.

The theoretical results for CPSK, shown in Fig. 7, are essentially the same as for NCFSK, except that the curves are shifted by approximately 4 dB to lower values of channel s/n. When speech was used in the simulation, the modulation being CPSK, the results are those shown in Fig. 8. The curves in this figure were shifted by approximately 2.5 dB to higher values of channel s/n compared to the theoretical curves. The deterioration in performance compared to the theoretical curves occurs because of the diverse nature of speech with its voiced

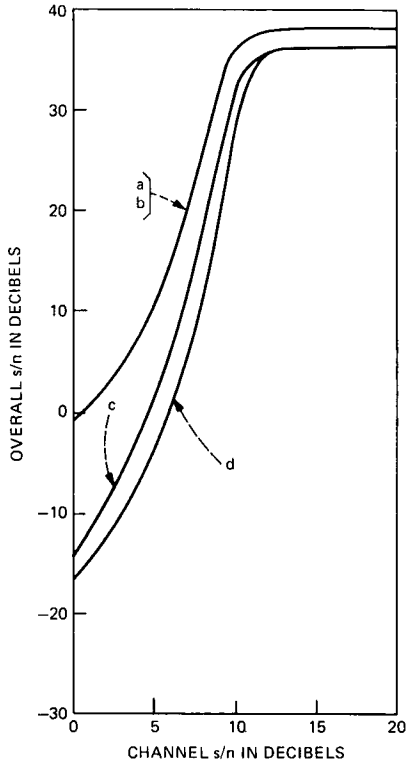

Fig. 7—Gaussian channel. Theoretical curves of overall s/n against channel s/n for CPSK modulation (a) −17 dB input power, MDC; (b) −17 dB input power, FBC; (c) −40 dB input power, MDC; and (d) −40 dB input power, FBC.

and unvoiced sections, and its intraword and interword silences. The theoretical curves apply to input signals having exponential PDFs, while speech is notorious for its nonstationary statistics. Nevertheless, sources having exponential PDFs are often used to represent speech, and clearly the theoretical and speech curves do have similar shapes, albeit their difference in absolute $\hat{s}/n$ for a given channel s/n. This curve similarity is particularly evident when we compare the performances of FBC and MDC at input levels of −17 and −40 dB.

7.2 Rayleigh fading channel

Figure 9 shows the variation of $\hat{s}/n$ as a function of channel s/n for a Rayleigh fading channel and for CPSK modulation. The theoretical curves in this figure relate to a number of conditions. For each of the two input power levels of −17 dB and −40 dB, we computed the curves for FBC and MDC when the bits were scrambled prior to transmission and when no scrambling was performed. The four curves, a, b, c, and

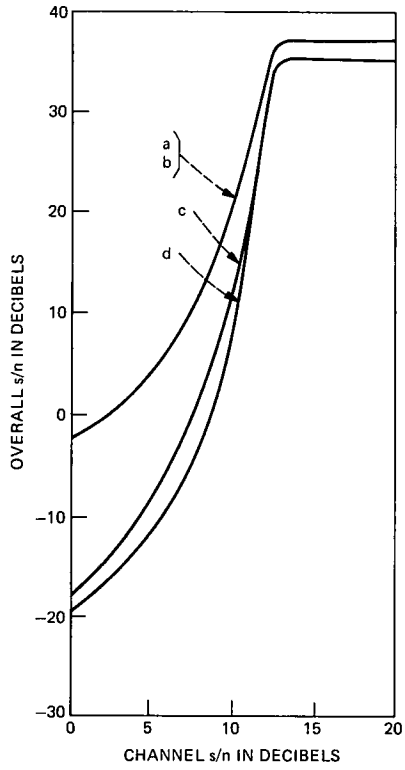

Fig. 8—Gaussian channel. Speech simulation curves of overall s/n against channel s/n for CPSK modulation (a) −17 dB input power, MDC; (b) −17 dB input power, FBC; (c) −40 dB input power, MDC; and (d) −40 dB input power, FBC.

d, coaleased for the input power of −17 dB. For a channel s/n of 30 dB, and the lower input power, MDC had a $\hat{s/n}$ advantage of 5 dB over FBC when bit scrambling was performed, and only a 0.8-dB gain in $\hat{s/n}$ in the absence of bit scrambling. We observed that MDC with bit scrambling, curve e, had a gain in $\hat{s/n}$ of 9 dB compared to curve h, where FBC without bit scrambling was employed. These gains in $\hat{s/n}$ are valid for channel s/n values where $\hat{s/n} > 0$ dB.

We also computed the theoretical curves for NCFSK, and we obtained curves that were almost identical to those shown in Fig. 9 but shifted by 6 dB to higher values of channel s/n. As with CPSK, over most of the range of channel s/n the curves are parallel, indicating that as the Bit Error Rate (BER) increases the relative performance of the different codes is unchanged.

7.2.1 PCM speech over mobile radio channels

The μ-law PCM encoded speech was allowed to two-level CPSK

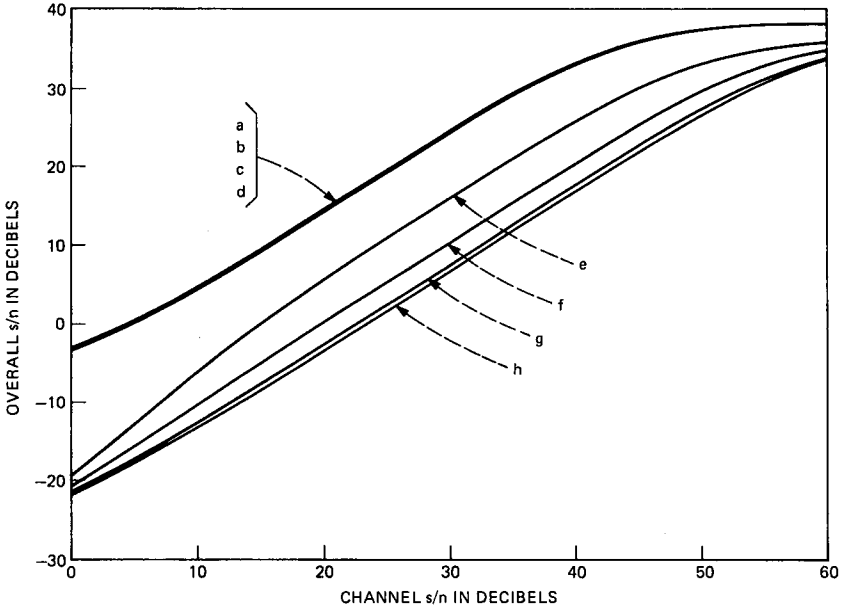

Fig. 9—Rayleigh fading channel. Theoretical curves of overall s/n against channel s/n for nondiversity CPSK modulation: (a) −17 dB input power, bit scrambling, MDC; (b) −17 dB input power, bit scrambling, FBC; (c) −17 dB input power, no bit scrambling, MDC; (d) −17 dB input power, no bit scrambling, FBC; (e) −40 dB input power, bit scrambling, MDC; (f) −40 dB input power, bit scrambling, FBC; (g) −40 dB input power, no bit scrambling, MDC; and (h) −40 dB input power, no bit scrambling, FBC.

modulate an RF carrier. A sequence of the envelope function $A(t)$ was generated from a hardware simulator of frequency-selective Rayleigh-fading mobile radio paths.[17] The $A(t)$ signal was sampled at 32 kHz and inserted into the computer to provide the fading envelope of a vehicle traveling at 15 mph. By resampling $A(t)$ we were able to produce fading envelopes for different vehicular speeds. The CPSK signal was subjected to these fading envelopes and corrupted by cochannel interference. The recovered baseband signal was sampled at the PCM bit rate to produce at the kth instant,[17]

$$B_k = R_k b_k + I_k, \tag{64}$$

where R_k, b_k, and I_k were the amplitudes of the Rayleigh envelope, transmitted bit, and additive interference level, respectively. The regenerated bit, $\hat{b}_k$, was a logical one if $B_k \geq 0$; otherwise it was a logical zero. The bits were grouped into PCM words and decoded using μ-law PCM. The difference between the input speech sequence and the decoded PCM sequence yielded the error sequence. The over s/n was then computed.

Figure 10 shows the variation of the $\hat{s}/n$ for our speech signal as a

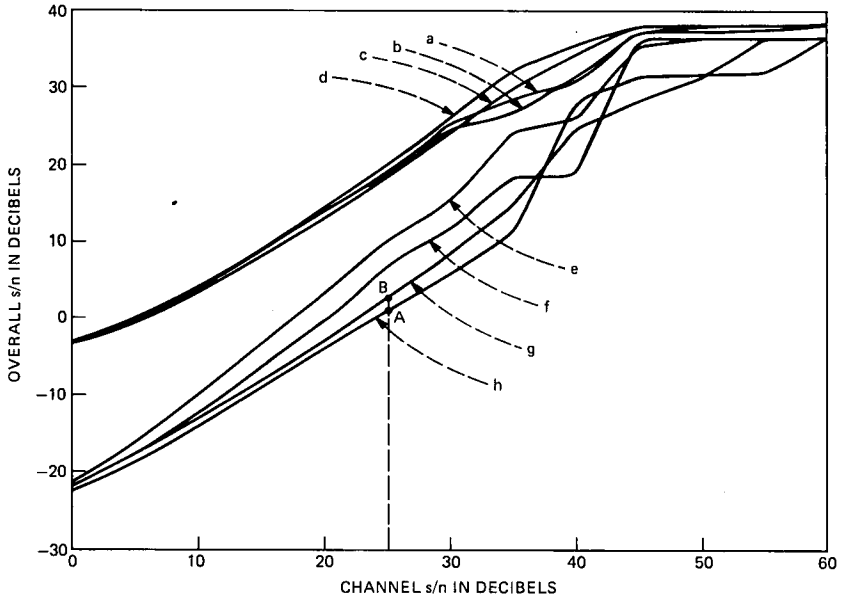

Fig. 10—Mobile radio channel. Speech simulation curves of overall s/n against channel s/n for nondiversity CPSK modulation with a vehicular speed of 30 mph. Curve labels are as in Fig. 9.

function of the channel s/n, for a vehicular speed of 30 mph. Eight curves are displayed corresponding to those used in Fig. 9. The curves of Fig. 10 have the same general shape as those of Fig. 9. We repeated our experiment for vehicular speeds of 60 mph, and overlaid the curves for this speed with those shown in Fig. 10. The fit for the high input levels was fairly exact, but for the −40 dB input level there were substantial discrepancies. Had we been able to take sufficiently long segments of speech and channel variations, our curves at −40 dB would have approached those in Fig. 9, subject to the inherent discrepancy that speech does not have the exponential distribution assumed for the theoretical case. The greater variations in the slopes of the curves of Fig. 10 compared to those in Fig. 9 at the −40 dB input level compared to the −17 dB level is to be expected, since for the same error rate the effect of an error can have a much greater influence on $\hat{s}/n$ when the input level is low.

We display in Fig. 11 a segment of the original input speech waveform, and the corresponding recovered waveforms obtained for conditions marked *A* and *B* in Fig. 10, respectively. The characteristic large error spikes associated with FBC are evident in Fig. 11b, where a spike can exceed half the amplitude range of the input speech signal. The nature of the MDC is to cause small spikes when the input speech

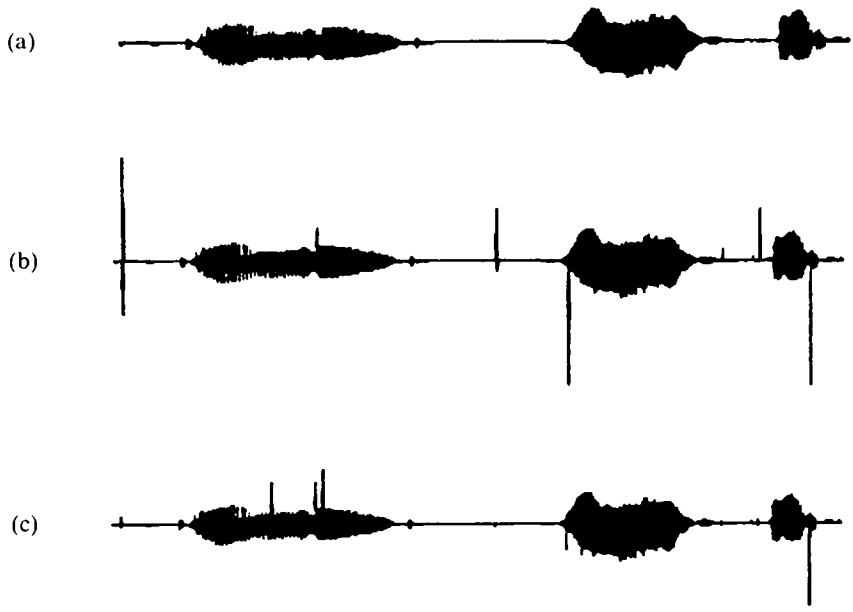

Fig. 11—μ-law PCM speech waveforms for mobile radio channels, nondiversity CPSK, vehicular speed 30 mph, −40 dB input power level, 25-dB channel s/n, and no bit scrambling: (a) original speech; (b) recovered speech with FBC (point A in Fig. 10); and (c) recovered speech with MDC (point B in Fig. 10).

samples are small, or indeed, when they are very large (see Table I and Fig. 11c). Errors in samples quantized to the middle of the range are responsible for the largest spikes with MDC.

7.2.2 Effect of diversity

When 2-branch ($M = 2$) diversity is applied, the value of $\hat{s/n}$ depends upon whether we use ideal maximum-ratio-combining diversity (IMRCD), or ideal selection-combining diversity (ISCD). Figure 12 displays the variation of $\hat{s/n}$ against channel s/n for numerous conditions, the modulation being CPSK. We observe that IMRCD is preferable to ISCD, that MDC coupled with bit scrambling is the best of our choices at the −40 dB input level, and that the curves have the same form as for $M = 1$ (see Fig. 9), except that the system can now operate at significantly lower values of channel s/n.

We do not show the theoretical curves for NCFSK for $M = 2$. Suffice it to say that they are virtually identical to those of CPSK, $M = 2$, except for a shift of 6 dB to higher values of channel s/n.

For the mobile radio channel described in Section 7.2.1 the curves of Fig. 13 were obtained. For reasons of clarity, we show only those curves with bit scrambling. These results are similar to those in Fig.

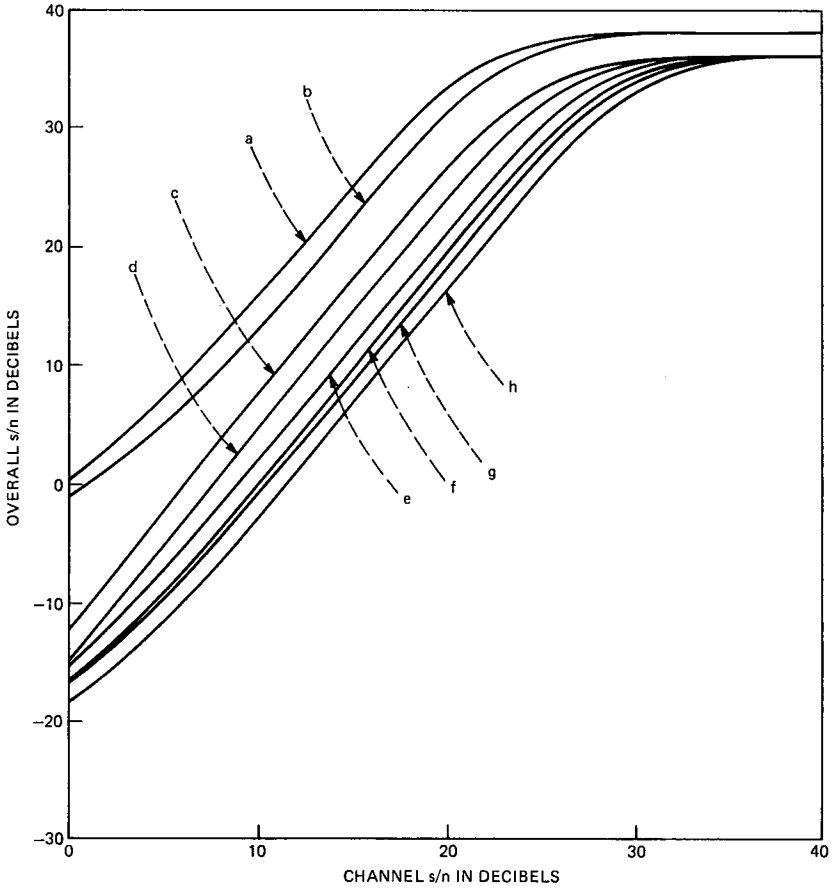

Fig. 12—Rayleigh fading channel (2-branch diversity). Theoretical curves of overall s/n against channel s/n for CPSK modulation: (a) −17 dB input power, IMRCD, bit scrambling and no bit scrambling, FBC, and MDC; (b) −17 dB input power, ISCD, bit scrambling and no bit scrambling, FBC, and MDC; (c) −40 dB input power, IMRCD, bit scrambling, MDC; (d) −40 dB input power, ISCD, bit scrambling, MDC; (e) −40 dB input power, IMRCD, bit scrambling, FBC, also no bit scrambling, MDC; (f) −40 dB input power, IMRCD, no bit scrambling, FBC; (g) −40 dB input power, ISCD, bit scrambling, FBC, also no bit scrambling, MDC; and (h) −40 dB input power, ISCD, no bit scrambling, FBC.

12, where the somewhat erratic behavior of the curves at the lower input power level is attributable to the reasons discussed in connection with the corresponding curves in Fig. 10.

The effect of using different values of M on the theoretical $\hat{s/n}$ is displayed in Fig. 14 for NCFSK, an input power level of −17 dB, MDC, bit scrambling, and IMRCD and ISCD. As M is increased, the knee of the curves moves to lower values of channel s/n, and the advantage of using IMRCD over ISCD increases. Figure 15 shows the

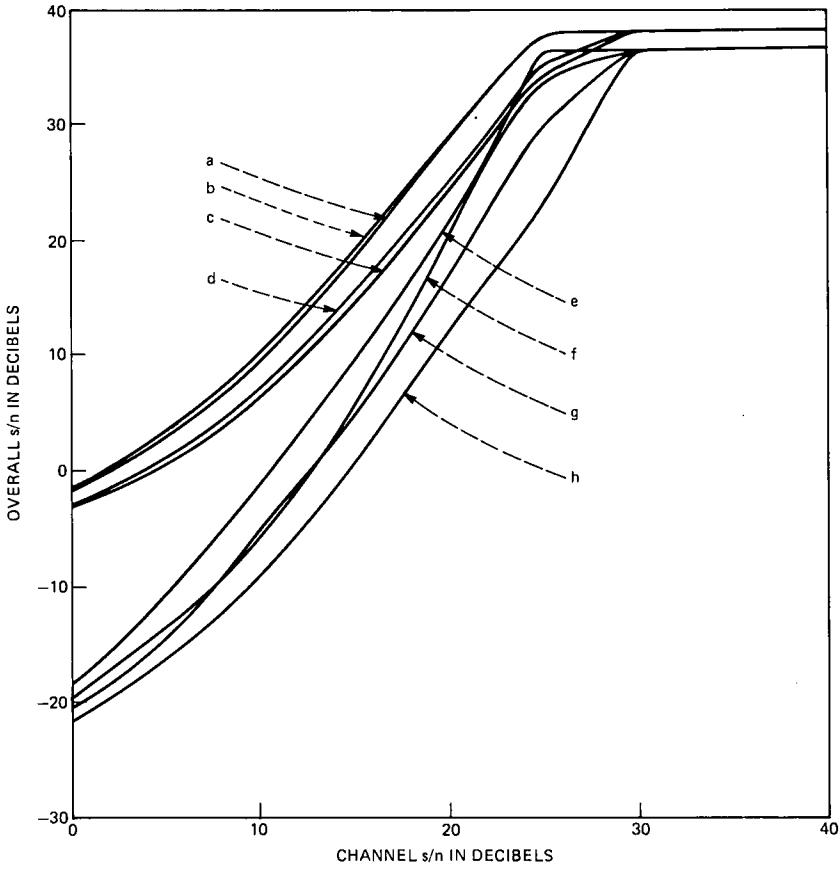

Fig. 13—Mobile radio channel. Speech simulation curves of overall s/n against channel s/n for CPSK modulation. The vehicular speed is 30 mph, with 2-branch diversity and bit scrambling employed: (a) −17 dB input power, IMRCD, MDC; (b) −17 dB input power, IMRCD, FBC; (c) −17 dB input power, ISCD, MDC; (d) −17 dB input power, ISCD, FBC; (e) −40 dB input power, IMRCD, MDC; (f) −40 dB input power, IMRCD, FBC; (g) −40 dB input power, ISCD, MDC; and (h) −40 dB input power, ISCD, FBC.

theoretical curves for the same conditions using CPSK instead of NCFSK. Again we note the close correspondence between the curves if a lateral shift in channel s/n is made.

VIII. DISCUSSION

Digital noise in μ-law PCM systems has been examined for both Gaussian and Rayleigh fading channels. Theoretical results for the digital noise power, i.e., the noise power in the decoded signal, have been presented for both NCFSK and CPSK modulation. Underpinning this theory is the application of the A-factors, and accordingly we have

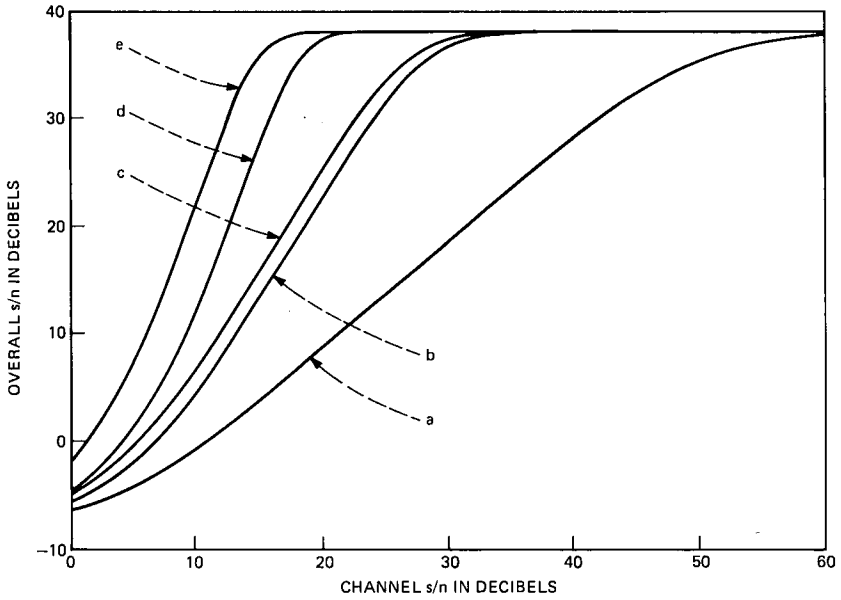

Fig. 14—Effect of diversity on Rayleigh fading channels. Theoretical cuves of overall s/n against channel s/n for −17 dB input power, NCFSK modulation, bit scrambling: (a) no diversity; (b) ISCD (M = 2); (c) IMRCD (M = 2); (d) ISCD (M = 4); and (e) IMRCD (M = 4).

elucidated their significance in detail. Armed with knowledge of the A-factors the determination of the digital noise power is greatly simplified [see eq. (9)]. We emphasize that although we have concentrated our attention on μ-law PCM, the A-factor approach is equally valid for A-law PCM. For this case the A-factors are computed by replacing the μ-law eqs. (29) and (30) by the A-law equations,[1,4] and proceeding as before.

Two binary codes for the μ-law PCM words were investigated: folded binary code (FBC) and minimum distance code (MDC). The MDC code yielded significant gains in s/n compared to FBC, with the proviso that the input power level was low. This is readily apparent upon inspection of Figs. 6 through 13. In our deliberations on Rayleigh fading channels we considered the effect of scrambling the bits in the PCM sequence prior to transmission, and compared it to the situation when bit scrambling was not employed. At low input power levels bit scrambling produced a gain of 8 dB when MDC was used, as shown in Fig. 9. The application of diversity made a significant contribution to system performance, and our best results occurred when we used a combination of ideal maximal-ratio-combining diversity, bit scrambling, and MDC binary code.

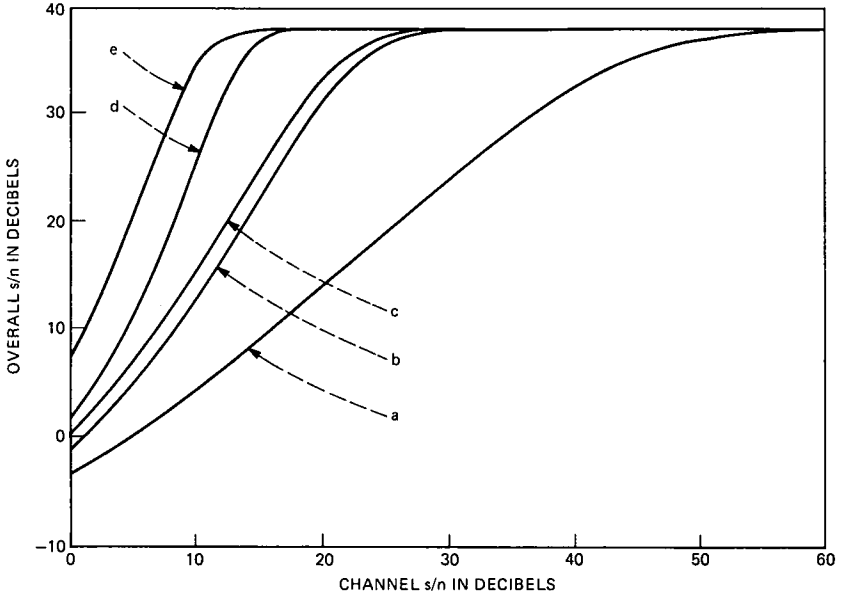

Fig. 15—Effect of diversity on Rayleigh fading channels. Same conditions as in Fig. 14, except that CPSK modulation is used.

Four concatenated sentences of speech were used in our simulations, and we have shown in our figures that there is consistency in the shape of the simulated and theoretical curves. In particular, at the higher input level the simulated and theoretical $\hat{s}/n$ values agree to within a couple of decibels, but for second-order diversity the discrepancy is $\simeq 4$ dB. These departures from the theory are a consequence of deriving our formulae for an input signal having an exponential PDF. Speech, by contrast, has time-varying statistics. However, voiced speech constitutes nearly 80 percent of speech, and its PDF can be approximated by an exponential one. It is for this reason that we used the exponential PDF in our theoretical deliberations.

REFERENCES

1. K. W. Cattermole, *Principles of Pulse Code Modulation*, London: Iliffe, 1969.
2. J. L. Flanagan, M. R. Schroeder, B. S. Atal, R. E. Crochiere, N. S. Jayant, and J. M. Tribolet, "Speech Coding," IEEE Trans. Commun., *COM-27* (April 1979), pp. 710–37.
3. N. Rydbeck and C.-E. Sundberg, "Analysis of Digital Errors in Non-Linear PCM Systems," IEEE Trans. Commun., *COM-24*, No. 1 (January 1976), pp. 59–65.
4. C.-E. Sundberg, "The Effect of Single Bit Errors in Standard Nonlinear PCM Systems," IEEE Trans. Commun., *COM-24*, No. 9 (September 1976), pp. 1062–4.
5. C.-E. Sundberg and N. Rydbeck, "Pulse Code Modulation With Error-Correcting Codes for TDMA Satellite Communication Systems," Ericsson Technics, *32*, No. 1 (1976), pp. 3–56.

6. N. Rydbeck and C.-E. Sundberg, "PCM/TDMA Satellite Communication Systems With Error-Correcting and Error-Detecting Codes," Ericsson Technics, *32*, No. 3 (1976), pp. 195–247.
7. E. Bedrosian, "Weighted PCM," IRE Trans. Inform. Theory, *IT-4* (March 1958), pp. 45–9.
8. C.-E. Sundberg, "Optimum Weighted PCM for Speech Signals," IEEE Trans. Commun., *COM-26*, No. 6 (June 1978), pp. 872–81.
9. C.-E. Sundberg, W. C. Wong, and R. Steele, "Weighting Strategies for Companded PCM Transmitted Over Rayleigh Fading and Gaussian Channels," AT&T Bell Lab. Tech. J, *63*, No 4 (April 1984), pp. 587–626.
10. R. Steele and D. J. Goodman, "Detection and Selective Smoothing of Transmission Errors in Linear PCM," B.S.T.J., *56*, No. 3 (March 1977), pp. 399–409.
11. R. Steele, "Partial Removal of Transmission Errors in Digitally Encoded Speech," Electronics and Power, *24*, No. 6 (June 1978), pp. 451–4.
12. C.-E. Sundberg, "Soft Decision Demodulation for PCM Encoding Speech Signals," IEEE Trans. Commun. *COM-26* (June 1978), pp. 854–9.
13. W. C. Y. Lee, *Mobile Communication Engineering*, New York: McGraw-Hill, 1982.
14. C.-E. Sundberg, "Block Error Probability for Non-Coherent FSK with Diversity for Very Slow Rayleigh Fading in Gaussian Noise," IEEE Trans. Commun., *COM-29*, No. 1 (January 1981), pp. 57–60.
15. A. P. Clark, *Principles of Digital Data Transmission*, London: Pentech Press, 1976.
16. D. J. Goodman and C.-E. Sundberg, "Transmission Errors and Forward Error Correction in Embedded Differential Pulse Code Modulation," B.S.T.J., *62*, No. 9 (November 1983), pp. 2735–64.
17. W. C. Wong, R. Steele, B. Glance, and D. Horn, "Time Diversity With Adaptive Error Detection to Combat Rayleigh Fading in Digital Mobile Radio," IEEE Trans. Commun., *COM-31*, No. 3 (March 1983), pp. 378–87.

AUTHORS

Raymond Steele, (SM '80), B.S. (Electrical Engineering) from Durham University, Durham, England, in 1959, the Ph.D. degree in 1975, and the Doctor of Science Degree (DSc) in 1983. Prior to his enrollment at Durham University, he was an indentured apprenticed Radio Engineer. After research and development posts at E. K. Cole Ltd., Cossor Radar and Electronics, Ltd., and The Marconi Company, all in Essex, England, he joined the lecturing staff at the Royal Naval College, Greenwich, London, England. Here he lectured in telecommunications to NATO and the External London University degree courses. His next post was as Senior Lecturer in the Electronic and Electrical Engineering Department of Loughborough University, Loughborough, Leics., England, where he directed a research group in digital encoding of speech and television signals. In 1975 his book, *Delta Modulation Systems* (Pentech Press, London), was published. He was a consultant to the Acoustics Research Department at Bell Laboratories in the summers of 1975, 1977, and 1978, and in 1979 he joined the company's Communications Methods Research Department, Crawford Hill Laboratory, Holmdel, N.J. In 1983 he became Professor of Communications in the Electronics Department at the University of Southampton, England.

Carl-Erik W. Sundberg, M.S.E.E., 1966, and Dr. Techn., 1975, Lund Institute of Technology, University of Lund, Sweden; Bell Laboratories, 1981–1982. Mr. Sundberg is an Associate Professor in the Department of Telecommunication Theory, University of Lund, and a consultant in his field. He is Director of the consulting company SUNCOM, Lund. During 1976 he was with the European Space Research and Technology Centre (ESTEC), Noordwijk, The Netherlands, as an ESA Research Fellow. He has been a Consulting Scientist at LM Ericsson and SAAB-SCANIA, Sweden, and at AT&T Bell Laboratories. His research interests include source coding, channel coding

(especially decoding techniques), digital modulation methods, fault-tolerant systems, digital mobile radio systems, spread spectrum systems, and digital satellite communication systems. He has published a large number of papers in these areas during the last few years. Senior Member, IEEE; member, SER, Sveriges Elektroingenjörers Riksförening.

Wai Choong (Lawrence) Wong, B.Sc.(Hons.) 1976, and Ph.D. 1980, in Electronic and Electrical Engineering, Loughborough University of Technology, U.K.; Bell Laboratories, 1980–83; from 1980 to 1983 Mr. Wong was with the Communications Methods Research Department at Bell Laboratories, working on speech enhancement, simultaneous transmission of speech and data, fading channel response modeling, and digital modulation techniques. In 1983 he joined the National University of Singapore as a lecturer. His current interests include digital speech and video signal processing, mobile radio communications, and digital modulation techniques.